

THE PROPERTIES OF THE FEL OUTPUT FOR SELF SEEDING

J. Bahrtdt, BESSY, Berlin, Bart Faatz, Rolf Treusch, Deutsches Elektronen-Synchrotron (DESY), Hamburg, Velizar Miltchev, Hamburg University (Uni HH) Institut fuer Experimentalphysik, Ruben Reininger, ruben@sas-rr.com.

Abstract

Several seeding schemes, like self seeding for FLASH or seeded HGHG cascades for BESSY soft X-ray FEL, are proposed for existing or planned free electron laser facilities. The simulation of these schemes requires the detailed knowledge of the properties of the seeding radiation and the implementation of these properties in the codes. Time dependent simulations with the 3D code GENESIS calculate the electric field distribution in and at the end of the undulator. The physical optics code PHASE permits the propagation of wave fronts across grazing incidence optics. Using the combination GENESIS PHASE GENESIS, the properties of the FEL output for different seeding schemes can be obtained. For example, the radiation quality of a SASE FEL can be improved in a self seeding scheme. Here, the radiation is monochromatized after a first undulator section and seeded to the second undulator modules. We present simulation studies for the self seeding option of FLASH.

INTRODUCTION

Synchrotron radiation beamlines at 3rd generation storage rings are generally optimized with ray tracing codes which are based on geometrical optics. This is justified as long as the radiation is incoherent. Coherent radiation has to be propagated with physical optic codes which describe the coherent properties of the light. FELs, the 4th generation light sources, are built to produce transversally and longitudinally coherent radiation in the wavelength regime down to 1Å.

X-ray FEL facilities based on the SASE principle are under construction at various places [1-3]. Since the SASE is a random process the longitudinal distribution of the light pulse as well as the spectrum is spiky.

Using a coherent seed pulse the FEL output can hence significantly be improved. The cascaded HGHG FEL scheme uses the coherent properties of the seed laser and transforms these properties through several stages to the required wavelength regime where no seeding laser is available [4,5]. The radiation properties degrade with the number of stages involved. Therefore, it is advantageous to start with a rather short seeding wavelength which can be produced by high harmonic generation (HHG) [6] in order to reduce the number of stages.

Self seeding is another approach to improve the spectral properties of the FEL [7]. The SASE radiation is passed through a monochromator which filters out the central frequency. This radiation is used as a seed for the following undulators.

It has also been shown that the output power of a cascaded HGHG FEL can be enhanced if the radiation of the first stage is monochromatized before transportation to the next one [8].

These examples demonstrate that there is no strict separation between FEL undulators and monochromators. They have to be described in a closed form, instead. In this paper we demonstrate for the example of the self seeding option of FLASH the necessity for a three dimensional and time dependent description of the propagating coherent radiation within the undulators and the monochromators.

THE PHYSICAL OPTICS CODE PHASE

The propagation of wavefronts in free space is usually done using Fourier optics techniques [9]. Depending on the geometry one of three propagators can be applied:

- i) In the near field approximation the electric field distribution is expanded in plane waves, the plane waves are propagated by multiplication with a complex factor and the result is back transformed to real space.
- ii) In the far field approximation the image distribution is composed of the contributions from individual point sources.
- iii) In the very far field the field distribution equals the angle distribution in the source plane (apart from a constant factor).

Optical elements can be introduced into this formalism in the following way: The electric field is propagated to the center of the optical element with Fourier optics. Then, the wavefront is propagated over the optical element using a ray tracing technique which takes into account the phase differences. Then, the wavefront is further propagated with Fourier optics methods (ZEMAX, GLAD [10,11]).

The code PHASE, written at BESSY, is based on another technique, the stationary phase approximation [12] which will be briefly explained.

The following equation correlates the electric fields in the source and the image plane.

$$\vec{E}(\vec{a}') = \int h(\vec{a}', \vec{a}) \cdot \vec{E}(\vec{a}) \cdot d\vec{a}$$

The integration is done over the source plane and the propagator \vec{h} has the form:

$$h(\vec{a}', \vec{a}) = \frac{1}{\lambda^2} \int_{Surface} \frac{\exp(ik(r+r'))}{rr'} \cdot b(w, l) \cdot \cos(\alpha) \cdot dw \cdot dl$$

r, r' are the distances between the source / image plane and the optical element, b is the obliquity factor

and the integration extends over the optical element surface. Each point in the image plane requires the evaluation of a four dimensional integral. Each additional optical element adds another two dimensions in the integral and it is obvious that the expressions can not be evaluated within reasonable time without certain assumptions. The stationary phase approximation uses the fact that the optical path length changes quadratically with the optical element coordinates in a region close to the principle rays (extremum of the optical path). The integration over the optical element coordinates can be done analytically if the beam is not scraped at that element and hence, the dimensions of the integral can be reduced from six to four.

All expressions (coordinates, path length, scaling factors etc.) are expanded up to fourth order in the coordinates and angles of the initial plane. Using these expansions the transformation of cross products of coordinates and angles can be derived as well. Using these cross terms the transformation over one element can be expressed via a 70x70 matrix. The combination of several optical elements is done simply by the multiplication of the individual matrices.

In principle the complete beamline can be described with one single matrix for each term as long as the photon beam does not hit an aperture. In case of a monochromator at least two runs are required: i) propagation from the initial plane to the exit slit and ii) propagation from the exit slit to the image plane.

Monochromatic light is assumed during the propagation. For time dependent simulations, the input data have to be Fourier transformed and the individual frequencies have to be propagated one after the other. The results are again Fourier transformed yielding the time dependent fields at the exit of the monochromator.

All equations have been derived with the algebraic code REDUCE [13] and the basic code has been produced automatically. For more details on the algorithm we refer to [12].

THE SELF SEEDING OPTION OF FLASH

The basic setup of the self seeding option is illustrated in Figure 1. It consists of two undulator stages separated by a magnetic chicane and a monochromator. The first undulator operates as a SASE FEL in the linear regime. After it the electrons are separated from the SASE radiation. The electron beam passes through the magnetic bypass that is used to remove the longitudinal charge density modulation (micro bunching). The radiation pulse is spectrally filtered in a high resolution grating monochromator and afterwards is superimposed with the electron beam at the entrance of the second undulator. Thus the monochromatic photon beam serves as a coherent radiation seed, which is amplified up to saturation in the second undulator. The self seeding technique increases the spectral brilliance significantly i.e. the output power of the seeded FEL is concentrated in a single line which is orders of magnitude narrower

than the spectrum of the conventional SASE FEL. The concept of the self seeding has the advantage that it is independent of any external radiation source and the seed is naturally synchronized with the electron bunch.

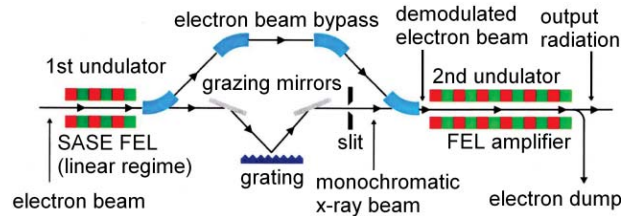


Figure 1: Schematic layout of the self seeding setup.

THE MONCHROMATOR

The seeding requirements for energy resolution, unity magnification, and only vertical deflections have been addressed [14] with a beamline (Figure 2) based on a spherical varied-line spacing grating (SVLSG).

The monochromator includes a plane mirror and three SVLSG (in the same spherical substrate) covering the energy range 6-64 nm. The plane mirror illuminates the grating at the correct angle of incidence such that the monochromator magnification is close to unity. In addition, each grating is designed to perfectly focus the beam along the dispersion (vertical) direction at the exit slit at two energies in its range, and to zero the coma aberration at one energy.

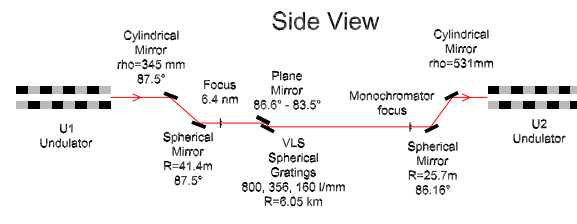


Figure 2: Seeding monochromator.

The pre and post focusing optics include four optical elements. The first and last optical components are two sagittally focusing cylinders that provide the unity magnification along the horizontal direction. The demagnification along the dispersion direction onto the entrance slit is performed with a spherical mirror. A spherical mirror after the exit slit magnifies the entrance slit width such that the size and divergence at the entrance of the second undulator overlaps with the electron beam for maximum amplification.

SIMULATIONS

Time dependent simulations for the first undulator at a carrier frequency of 60nm have been performed using GENESIS [15]. The standard FLASH undulator geometry has been assumed, where the electron beam is kicked in order to avoid saturation within the 15m undulator length which is required for shorter

wavelengths [16]. The total length over which the SASE interaction takes place is about 6.5 m, which is enough to reach a power level of about 0.2 GW. This value is well below saturation, but high enough to guarantee that after monochromatization the power is several orders of magnitude above shot noise. Electric fields for 560 slices (121x121 grid points) separated by 540nm provide the full information of the radiation pulse. The frequency resolution after Fourier transformation is determined by the length of the total pulse to be transformed. For a reasonable resolution the pulse length has been enlarged to 4096 slices by adding slices with no intensity.

After Fourier transformation the frequency slice for the central frequency (60nm) has been propagated upstream to find the beam waist. For this specific case the waist is located 1000mm upstream of the undulator exit.

The PHASE propagation has been limited to 40 frequencies. The other frequencies are diffracted by the grating to large angles such that they are blocked by the exit slit. The wavefronts corresponding to the 40 frequencies have been propagated to a plane close to the first element which is the initial plane for the subsequent PHASE propagation. The PHASE simulations have been done in two steps. First, the electric fields in the exit slit plane have been evaluated on a grid with 51x51 data points. The sizes of the slit aperture was chosen to be 2mm horizontally and 40 μ m, 200 μ m and 400 μ m vertically. These data have then been used in a second PHASE run from the exit plane to the center of the second undulator (2500mm downstream of the undulator entrance).

These 40 frequency slices plus the other 4096-40 frequency slices (the latter ones with no intensity) have been Fourier transformed to time space to be used in further GENESIS simulations through the second undulator. For this a modified version of GENESIS is used in order to include the full 6x6 matrix to describe the electron bypass that debunches the electron beam. The electric fields behind the monochromator have been scaled such that the intensity at the central frequency has dropped to 11 percent corresponding to the theoretical beamline transmission.

Figure 3 shows the temporal and spectral power of the initial pulse and the pulses behind the monochromator. Though the line width behind the monochromator shrinks with the slit width, the pulse duration does not increase.

The reason is the correlation between the wavelength and the spot location in the dispersion plane of the grating which is imaged to the center of the second undulator. The bandwidth at a certain grid point does not scale with the slit width because only a small frequency interval contributes to the intensity at that point.

For the simulation of the second undulator, the particle distribution of the first undulator is taken, which is debunched, using the full 6x6 matrix which has been simulated with ELEGANT. The field used as a seed is the one as calculated by PHASE. The total interaction

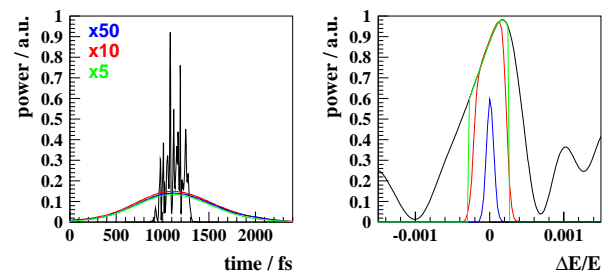


Figure 3: Relative power versus time (left) and frequency (right) for the initial pulse at the exit of the first undulator (black) and behind the monochromator for exit slits of 40 μ m (blue), 200 μ m (red) and 400 μ m (green). The monochromator transmission is not yet included.

length simulated is about 4.3 m, after which maximum peak brilliance has been reached.

RESULTS

The simulations for the three different slits show similar results. The main difference is that the seed power is different at the entrance of the second undulator. However, in all cases it is well above shotnoise and only influences the position at which saturation is achieved. In Figures 4 and 5, the results for a 400 μ m slit are shown.

Wider monochromator slits increase the total power which is, however, not completely passed to the electron beam because the transverse beam size acts as further slit. The spectral power increases by a factor of 2.5 going from 40 to 200 μ m slit width and does not increase further at 400 μ m.

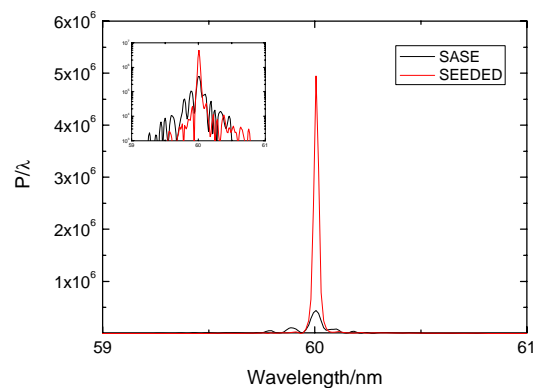


Figure 4: Comparison of the power spectrum for SASE (black curve) and a seeded pulse (red curve) for a slit of 400 μ m. The small graph in the top left corner shows the same spectrum on a logarithmic scale. Note that the central frequency of 60 nm for the seeded pulse is about an order of magnitude higher compared to SASE, whereas the other peaks are about a factor of 5 lower.

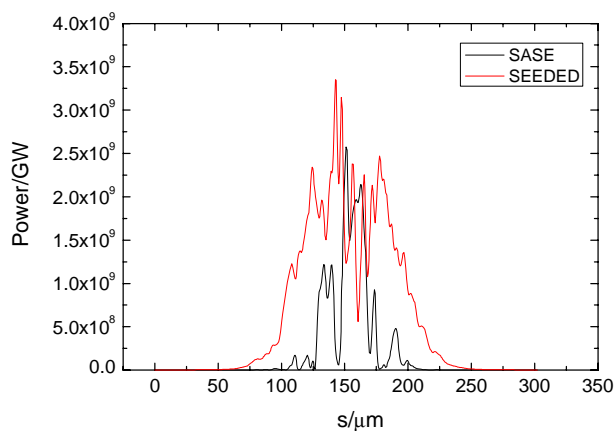


Figure 5: Power along the bunch for a SASE pulse (black curve) and the seeded pulse (red curve). Note that the seeded pulse is much smoother. The remaining spikes are at least partially due to the fact that the bunching is not fully suppressed in the simulation due to the limited number of particles used.

CONCLUSION

We presented for the first time combined time dependent FEL simulations and physical optics wavefront propagations using the codes GENESIS and PHASE. The wavefronts generated in a time dependent simulation of GENESIS have been propagated with the physical optics code PHASE and the result has been used as a seed for a further GENESIS run. It has been demonstrated that the self seeding scheme significantly improves the spectral performance of FLASH. The line width becomes narrower, the power increases and the temporal structure is smoother.

ACKNOWLEDGEMENT

We thank A. Meseck for adapting the code GENESIS and for many fruitful discussions.

REFERENCES

- [1] TESLA-Technical Design Report, TESLA X-FEL, Technical Design Report, 2002-9, 2002.
- [2] Linac Coherent Light Source (LCLS), Conceptual Design Report, SLAC-R-593, 2002.
- [3] T. Shintake, Nucl. Instr. and Meth., A507 (2003) 382-397.
- [4] L. H. Yu, NIM A, 483 (2002) pp493-498.
- [5] X. J. Wang et al., DUV, Proceedings of the 26th International FEL Conference, Trieste, Italy, 2004, pp 209-211.
C. Bochetta et al., FERMI, Proceedings of the 27th International FEL Conference, Stanford, CA, 2005, pp 632-685.
The BESSY Soft X-ray Free Electron Laser, Technical Design Report March 2004, eds.: D. Krämer, E. Jaeschke, W. Eberhardt, ISBN 3-9809534-08, BESSY, Berlin (2004).
- [6] M.-E. Cuprie et al., ARC-EN-CIEL, Proceedings of the 27th International FEL Conference, Stanford, CA, 2005, pp.55-58.
A. Andersson et al., MAX IV, Proceedings of the 26th International FEL Conference, Trieste, Italy, 2004, pp 190-192.
D. Wang et al., MIT, Proceedings of 2005 PAC, Knoxville, Tennessee, pp1961-1963.
J. Wu, Z. Huang, LCLS, Proceedings of the 27th International FEL Conference, Stanford, CA, 2005.
Gullens et al., LBNL, Proceedings of the EPAC 2006, Edinburgh, Scotland, pp 142-144.
J. Qi-ka et al., SDUV, Proceedings of the 26th International FEL Conference, Trieste, Italy, 2004, pp 494-497.
- [6] O. Tscherbakoff et al., Proceedings of the EPAC 2006, SPARC, Edinburgh, Scotland, pp 47-49.
G. Lambert et al., SCSS, Proceedings of the EPAC 2006, Edinburgh, Scotland, pp 44-46.
J. A. Clarke, 4GLS, Proceedings of the EPAC 2006, Edinburgh, Scotland, pp 181-183.
- [7] J. Feldhaus et.al., Opt. Commun., 140 (1997), 341.
- [8] K. Goldammer et al, Proceedings of the 27th International FEL Conference, Stanford, CA, 2005, pp.23-26.
M. Abo-Bakr et al., Proceedings of the 27th International FEL Conference, Stanford, CA, 2005, pp.19-22.
- [9] J. W. Goodman, "Introduction to Fourier Optics", McGraw-Hill Physical and Quantum Electronics Series, New York, 1968.
- [10] GLAD, Theory Manual, Applied Optics Research, 1087 Lewis River Road, 217 Woodland, WA, 2004.
- [11] ZEMAX, Optical Design Program, User's Manual, ZEMAX Development Corporation, November 2005.
- [12] J. Bahrtdt, Applied Optics, 34 (1995) 114-127.
J. Bahrtdt, Applied Optics, 36 (1997) 4367-4381.
J. Bahrtdt, Proceedings of the 27th International FEL Conference, Stanford, CA, 2005, pp694-701.
- [13] A. C. Hearn, "REDUCE 3.5, A General Purpose Algebra System" [RAND, Santa Monica, Calif. 90407-2138 (reduce@rand.org), 1993].
- [14] R. Reininger, J. Feldhaus, P. Gürtler, and J. Bahrtdt, Nucl. Instr. Methods A, **467**, 38-41, 2001
- [15] S. Reiche, GENESIS 1.3, Nucl. Instr. Meth. A 429 (1999) 243.
- [16] V. Miltchev, "Simulation studies on the self seeding option at FLASH", presented at this conference.